J Mater Sci (2007) 42:3573–3579
DOI 10.1007/s10853-006-0167-8

Acoustic emission inspection of Portevin-Le Chatelier effect and deformation mechanisms of two Mg–Li–Al alloys

Cong Wang · Zhuoqun Li · Yongbo Xu · Enhou Han

Received: 20 December 2005 / Accepted: 3 April 2006 / Published online: 30 January 2007

Abstract In this paper, Portevin-Le Chatelier (PLC) effect of LA41 magnesium alloy is reported. With increasing strain rate, both ultimate tensile stresses (σ_b) and 0.2% proof ($\sigma_{0.2}$) stresses increase, while serrations become less severe. Major acoustic emission (AE) peaks appear at the end of elastic region, and transform to burst type signals in the plastic range. In another alloy containing less Li (LA11), serrations are absent and major AE peak values are considerably lowered. Additionally, PLC effect disappears in LA41 after annealing. The role of twins is discussed in details. Actual causes for AE activity during deformation are also proposed.

Introduction

The Portevin-Le Chatelier (PLC) effect was firstly discovered in mild steels deformed at elevated temperature [1]. Since then, similar results, usually elucidated by the model of dynamic strain aging (DSA), have been reported and studied exhaustively in other alloy systems.

C. Wang (✉) · Z. Li · E. Han
Environmental Corrosion Center, Institute of Metal Research, Chinese Academy of Sciences, Shenyang 110016, P.R. China
e-mail: congwang@imr.ac.cn

Y. Xu
Shenyang National Laboratory for Material Science, Institute of Metal Research, Chinese Academy of Sciences, Shenyang 110016, P.R. China

The classical DSA model, referring to the repeated pinning and unpinning of dislocations due to their interaction with diffusing solute atoms, was proposed by Cottrell and Bilby [2] and was advanced by McCormick [3] and van den Beukel [4, 5]. However, their treatments were derived from interactions between single mobile dislocation and diffusing solute atoms. Obviously, the onset of the PLC effect must be initiated by the simultaneous movement of an ensemble of mobile dislocations. Based on the collective behavior of dislocations, Korbel [6] and Schoeck [7] developed a modified model, leading to the PLC effect. Macroscopically, spatial and temporal behaviors of the PLC effect were also examined comprehensively. Kovacs et al. [8] investigated localization of plastic deformation associated to the PLC effect under constant stress rates. Lebyodkin et al. [9] studied the statistical distributions of the stress amplitudes both experimentally and theoretically in polycrystalline and single Al–Mg alloys. Hahner et al. [10] and Chihab et al. [11] put their emphasis on the theoretical modeling of kinetics of PLC bands.

Acoustic emission (AE), which refers to stress waves produced by sudden movement within a stressed material, is frequently observed during deformation of metals and alloys [12]. Though a lot of mechanisms account for deformation AE activity, AE created by slip (dislocation movement) and twinning are of great interests to materials scientists. AE can be affected by a number of intrinsic and extrinsic factors, such as chemical composition, strain rate, temperature and prior heat-treatment. As a consequence, AE inspection assumes as a powerful tool for examination on plastic deformation process because of the detailed and immediate information it provides. In particular,

groups led by Estrin [13], Carpenter [14], Lukac [15, 16] and Kainer [17–20] thoroughly investigated AE during plastic deformation of magnesium alloys. Therefore, AE is an excellent way of studying dynamic processes associated with plastic deformation of magnesium alloys. What deserves a mention here is that AE has been successfully used to investigate the PLC effect [16, 17] and stress drops are always accompanied by corresponding large AE bursts. To a certain degree, a correlation between AE activity and the PLC effect, which is associated with collective movement of mobile dislocations, can be easily drawn.

In this paper, mechanical properties of investigated alloys are reported and discussed in details. The aim is to reveal the relationships between PLC effect and AE responses under different strain rates. Potential mechanisms for deformation and microstructural differences are also proposed.

Experimental

Two Mg–Li–Al alloys, LA11 and LA41, were prepared by extrusion at the temperature of 623K with an extrusion ratio of 1:8. Then they were homogenized at 623K for 1\,h. The chemical compositions of these alloys are listed in Table 1. Tensile specimens with gauge dimensions of 30 mm × 10 mm × 5 mm were cut parallel to the extruded direction. Four LA41 specimens were annealed for 240 h at 523K. Uni-axial tensile testing was performed using an Instron 8562 servo-mechanical machine. All specimens were stretched in ambient air (Room Temperature) and at constant cross-head velocities of 0.6mm × min^{-1} (fast), 0.2mm × min^{-1} (medium) and 0.04mm × min^{-1} (slow), which are equivalent to initial strain rates of $3.33 \times 10^{-4}s^{-1}$, $1.11 \times 10^{-4}s^{-1}$ and $2.22 \times 10^{-5}s^{-1}$ respectively. Two piezoelectric transducers (PAC WD), which have bandwidth of 20–1,000 kHz and built-in preamplifiers bearing a gain of 30 dB, were attached symmetrically on the polished surfaces using silicon grease just outside the gauge length to avoid relative movement between the sensor and the specimen. All of the important data, including counts, hits, V_{rms} (root mean square voltage of the AE signals over a time interval) as well as load and time were attained by a 2-channel digital AE workstation acquisition system (PAC DiSP). Values of load and time were converted into nominal stresses and nominal strains correspondingly. The threshold was maintained at the value of 30 dB. The dead time was 1,000 μs.

Table 1 Chemical compositions of the employed alloys (in weight percent)

	Li	Al	Mg
LA11	1.22	0.91	Balance
LA41	4.32	0.97	Balance

Microstructural examination was carried out on an environmental scanning electron microscope (ESEM) under the acceleration voltage of 10 kV. The employed etchant was 3 g picric + 10 ml distilled water + 10 ml acid + 50 ml ethanol with etching time as high as 30 s. The samples for Transmission electron microscope (TEM) were spark-cut from alloy plates with the thickness of 0.6 mm. After being ground parallel to 50 μm thick, they were punched to discs with diameters of 3 mm. Finally, the foils for TEM were thinned electronically in a solution of 30 ml nitric + 70 ml methanol with a twin jet electro-polisher. Being rinsed for several times in pure ethanol, these foils were stored in a hermetic vacuum container. TEM observations were completed on a JEM 2000FXII TEM operated at the voltage of 200 kV.

Results

Microstructure characterization

Typical microstructures of the as-received LA11 and LA41 are presented in Fig. 1. The grains are homogenized, and no twins and precipitates are observed. Grain sizes of the two alloys are about 60 μm and 100 μm, respectively. Microstructures of the deformed specimens that twins are produced (Fig. 2). However, compared with as-received LA41, annealed ones exhibits entirely different micro-structural features (Fig. 3). Lens-like twins are created and distributed profusely. Short twins are probably newly born, while long twins are fully grown-up. They often appear in multiple parallel groups with some intersecting ones. Following TEM examination corroborates this point (Fig. 4). Generally, twins, induced either by tension or annealing, always end in sharp points close to grain boundaries (GBs).

As-received LA41

Figure 5 is the AE responses of as-received LA41 deformed at three different strain rates. These three stress–strain curves share the same appearance, with linear-plastic region, strain-hardening regime and stress plateau, indicating deformation mechanism does not change in the applied strain rate range. Stress–strain curves become serrated after incubation strains, which are the most appealing features of PLC effect.

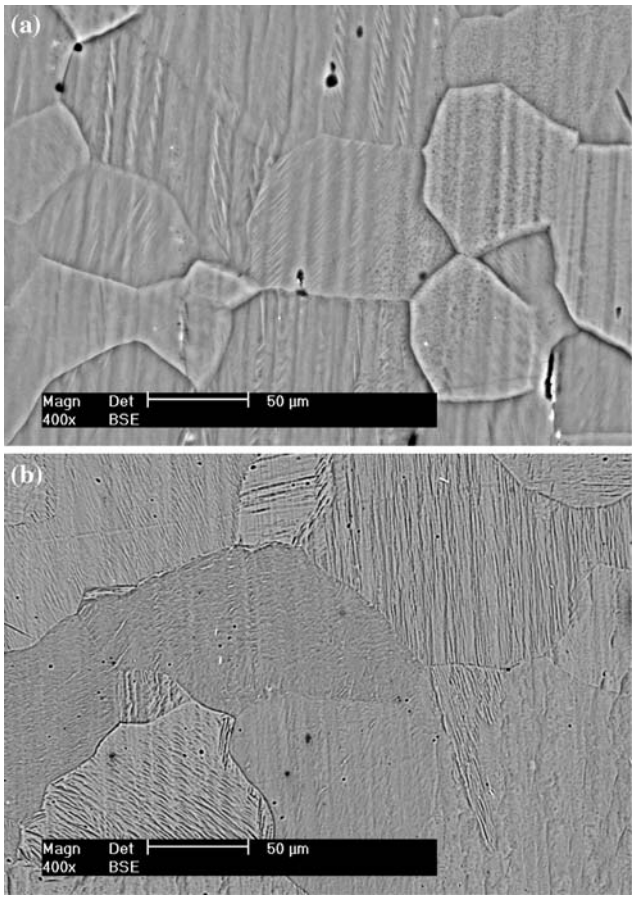

Fig. 1 Microstructures of as-received (**a**) LA41 and (**b**) LA11

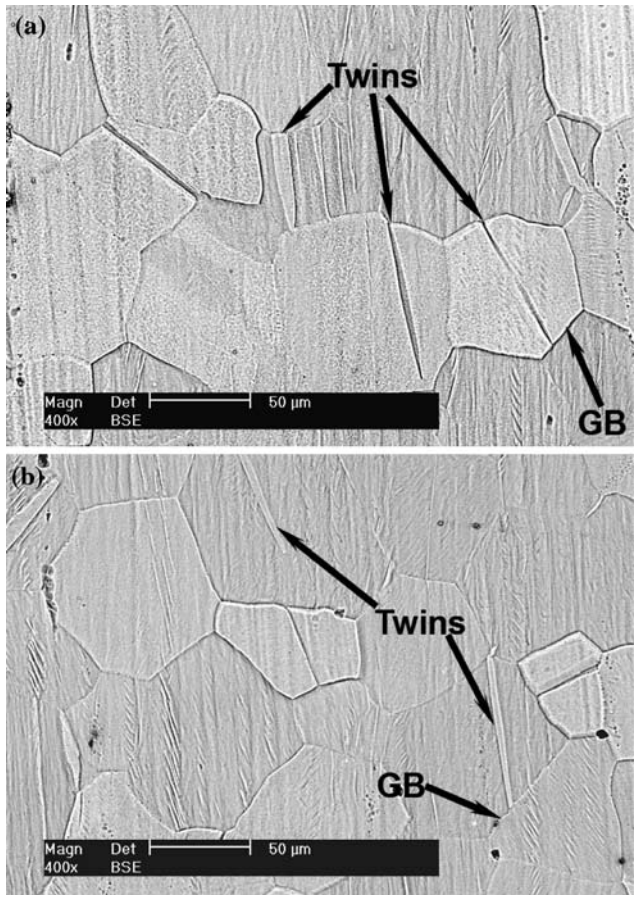

Fig. 2 Cross sections deformed to fracture of as-received (**a**) LA41 and (**b**) LA11

With increasing strain rate, serrations become less severe, while both the ultimate tensile stresses (σ_b) and 0.2% proof stresses ($\sigma_{0.2}$)increase a little (Fig. 6), giving rise to positive strain rate sensitivity (SRS). This point is contrary to classical DSA model for the onset of PLC effect because the DSA model demands that SRS should be negative when PLC effect becomes predominant [21].

A major AE peak always appears shortly after the yielding point. This can be explained by means of collective multiplication and propagation of massive dislocations in the vicinity of the yielding point. Careful examination, however, shows that dependence of V_{rms} on $\dot{\varepsilon}^{1/2}$ does not follow a linear relationship (Fig. 7). Since deformation mechanism is not altered with the applied strain rate change, twinning must take place during the deformation process. Following minor AE bursts are firmly associated with serrations. Obviously, during the process of DSA, mobile dislocations, temporarily arrested at obstacles, are released suddenly, rendering a sharp AE response possible. This confirms a former conclusion [22] that the AE activity is not proportional to the mobile dislocation density, but is closely associated with the conversion of immobile dislocations to mobile ones.

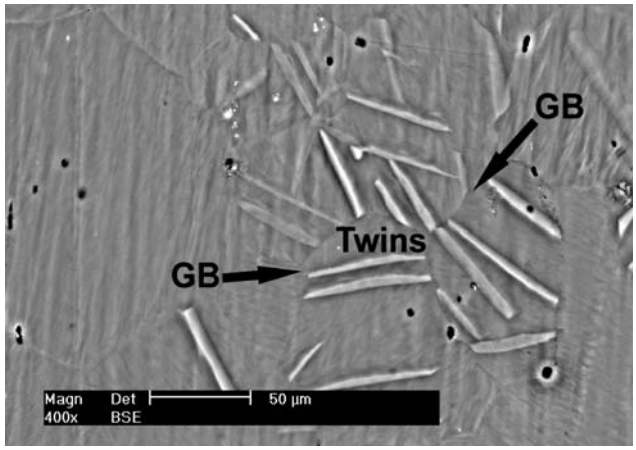

Fig. 3 Microstructure of annealed LA41with intersecting twins parallel twins

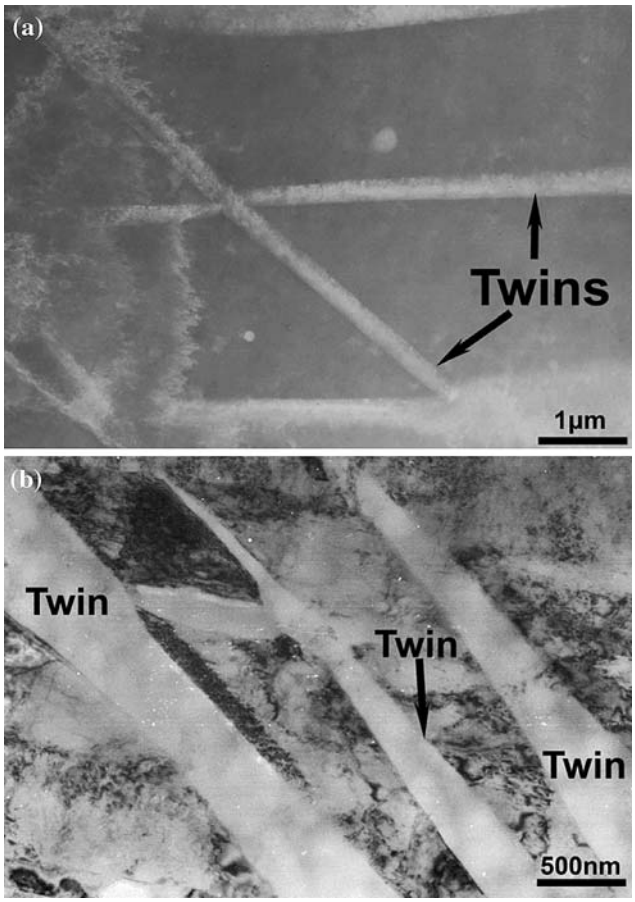

Fig. 4 Bright field (BF) morphology of annealed LA41 (**a**) intersecting twins and (**b**) parallel twins

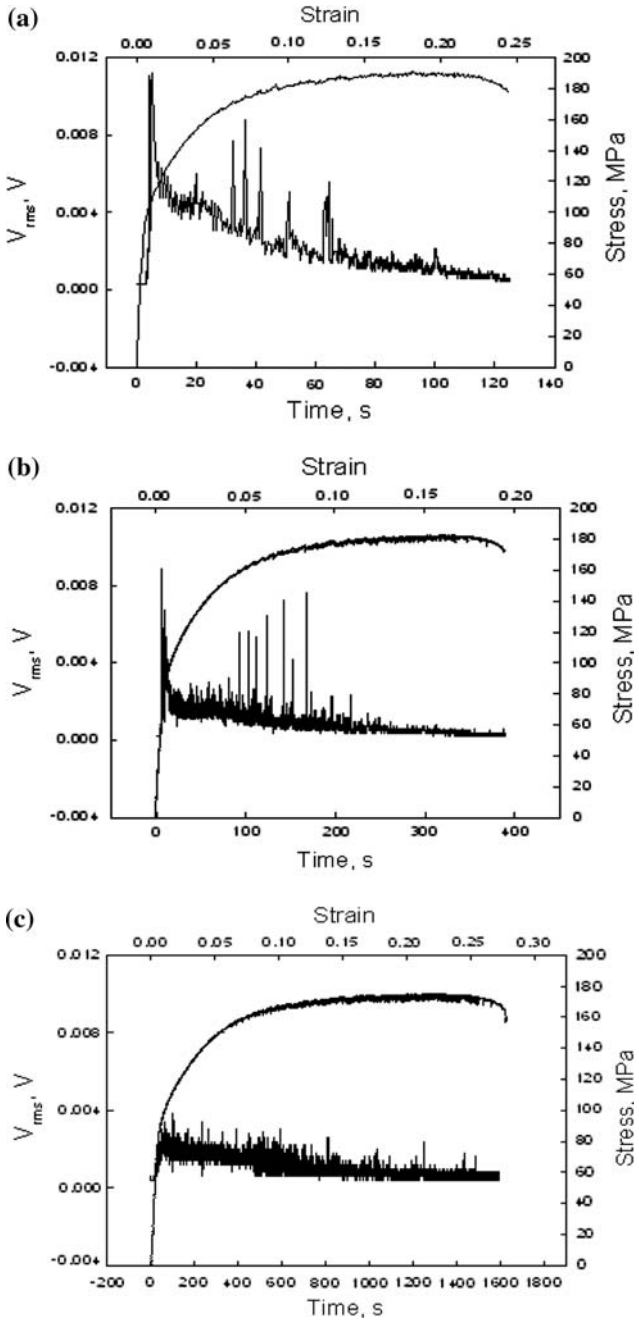

Fig. 5 Stress–strain curves and AE responses of as-received LA41under three different strain rates (**a**) $3.33 \times 10^{-4}s^{-1}$, (**b**) $1.11 \times 10^{-4}s^{-1}$ and (**c**) $2.22 \times 10^{-5}s^{-1}$

As-received LA11

Stress–strain curves and corresponding AE responses of as-received LA11 are presented in Fig. 8. Apparently, stress–strain curves remain smooth throughout deformation history, indicating that the PLC effect is absent in this alloy. The peak values of V_{rms} also exhibit a similar increasing tendency when strain rate is elevated though linear relationship cannot be satisfied. It should be noted that the AE peak values of LA11 are smaller than those of LA41, indicating that twinning and slip systems are difficult to provoke because of its lower Li content and associating higher ratio of *c*/*a*.

Annealed LA41

Figure 9 shows the stress–strain curve and AE response of annealed LA41 deformed at the strain rate of $1.11 \times 10^{-4}s^{-1}$. The stress–strain curve is smooth and the AE peak value is only half of as-received LA41 deformed at the same strain rate. From microstructure information provided above, it could be concluded that twins created after annealing might play an important role. It might be envisioned that annealing-induced twins obstruct normal movement of mobile dislocations and DSA may not be operative.

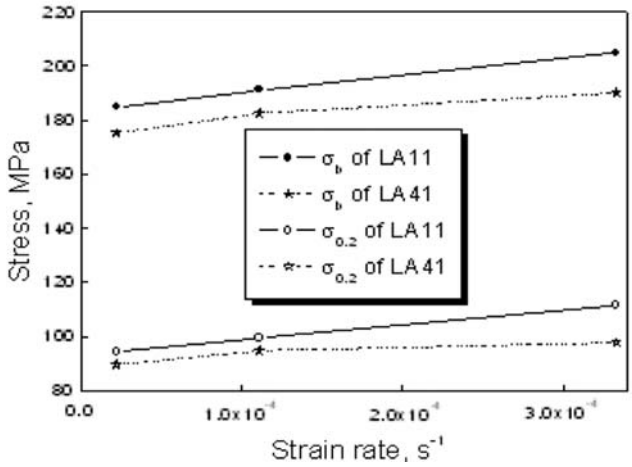

Fig. 6 Variations of σ_b and $\sigma_{0.2}$ with strain rate of as-received LA41 and LA11

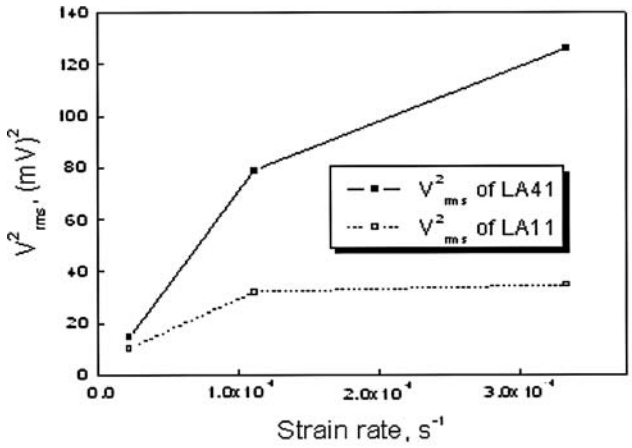

Fig. 7 Dependence of V_{rms} on strain rate of as-received LA41 and LA11

Discussions

Major AE peaks

AE peak value is achieved when the yielding point is reached. Such phenomenon provides the information that AE is most active in the vicinity of yielding point. At the beginning of deformation, both basal slip system, the easiest way of deformation for Mg-based alloys, and the potential prismatic slip, which offers additional independent slip mode, are easily initiated. In addition, Mg–Li alloys, with its *c*/*a* axial ratio less than 1.633, produce twins easily under tensile deformation [23]. Therefore, deformation twinning, which brings about burst type AE signals [24], will be activated during tension. The combination of these three deformation mechanisms surely makes intensive AE response possible. Thereafter, forest dislocations are exponentially created and the free length and flight distance of mobile dislocations are greatly reduced and AE is suppressed accordingly. That is to say, peak values of AE are confined around the neighborhood of yielding point and subsequent values of V_{rms} will decrease drastically.

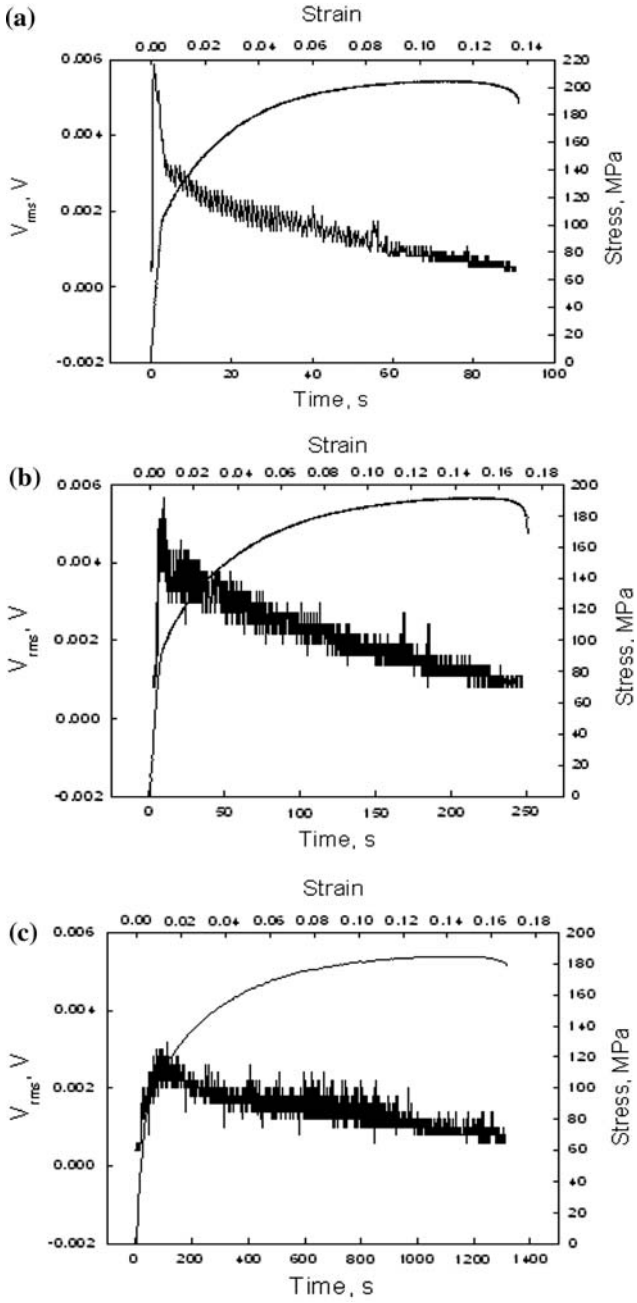

Fig. 8 Stress–strain curves and AE responses of as-received LA11 under three different strain rates (**a**) $3.33 \times 10^{-4}s^{-1}$, (**b**) $1.11 \times 10^{-4}s^{-1}$ and (**c**) $2.22 \times 10^{-5}s^{-1}$

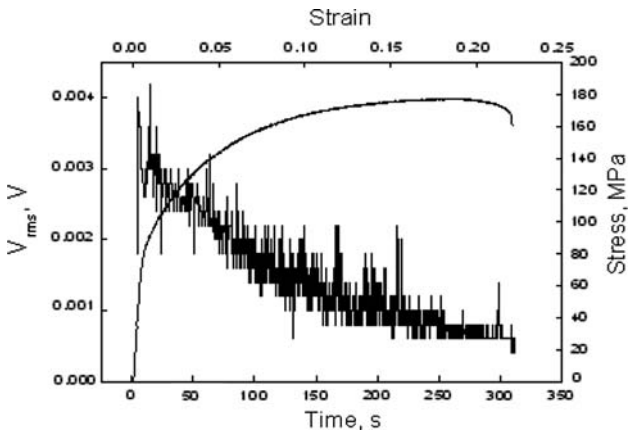

Fig. 9 Stress–strain curve and AE response of annealed LA41 under the strain rates of $1.11 \times 10^{-4}s^{-1}$

As pointed out by Fisher and Lally [25], if the mechanism responsible for producing AE is not changed in the strain rate, V_{rms} should be proportional to $\dot{\varepsilon}^{1/2}$. Because twinning is dependent on the strain rate, if a deformation process is dominated by the combination of slip and twinning, the above-mentioned relationship cannot be satisfied. In other words, twinning should be fully considered when complex deformation mechanisms are operative. As a matter of fact, because deformation twinning in as-received LA41 and LA11 did take place during tension, it is natural that the linear relationship between V_{rms} and $\dot{\varepsilon}^{1/2}$ cannot be satisfied.

Difference of lithium contents might shed some light on different AE responses of as-received LA41 and as-received LA11. The axial ratio of Mg will decrease continuously from 1.624 to 1.607 as a function of Li addition. Hauser et al. [26] pointed out that changes of axial ratio are primarily associated with a decrease in the (0002) lattice spacing rather than an increase in the $(10\bar{1}0)$ planar spacing. It is argued that prismatic slip system will be activated due to reduced Peierls stress. Therefore, prismatic slip of LA41 is much easily provoked than that of LA11, though critical resolved shear stresses (CRSS) of basal slip system of the two alloys are almost identical. More slip systems, to certain extent, are equivalent to more AE sources. As a result, AE peak values of as-received LA41 are much higher than those of LA11.

Minor AE bursts

Actual cause for the onset of continuous serrations in LA41 is discussed thoroughly by means of DSA [27]. Briefly, mobile dislocations are always arrested by obstacles such as forest dislocations. During the time when they stay at obstacles, solute atoms, say, Li and Al atoms will diffuse to mobile dislocations through pipe-diffusion mechanism. Such pinning will exert an extra force, which is corresponding to sudden stress increase, for mobile dislocations to overcome. However, when the deformation proceeds, arrested dislocations ought to be released from time to time, and the above-mentioned process will rehearse itself automatically, implying repetitive serrations on stress–strain curves. Obviously, this process involves the collective conversion of immobile (temporarily arrested) dislocations to mobile ones. Since intense AE is originated from the above-mentioned conversion [22], a few minor AE bursts will ensue as large strain is achieved.

The role of twins

Deformation induced twins

Generally speaking, magnesium and its alloys do not exhibit good plasticity because under usual circumstances only three basal slip systems are operative. The von Mises criterion [28] cannot be satisfied due to limited slip systems. Therefore, activation of twinning, primarily in $(10\bar{1}2)$ plane, is necessary for homogeneous plastic deformation. Deformation twinning always brings about burst type AE signals [24]. By employing deformation twinning, Friesel and Carpenter [14] successfully AE bursts in AZ31B magnesium alloys during tension. Mathis [15] ascribed intensive AE signals of AM60 to high density of twins. Based on systematic experiment on AZ family, Bohlen [18] concluded that twinning constituted one of the most essential sources for AE.

From microscopic observations given above, it may be concluded that deformation twinning of as-received LA41 and LA11 contribute much to their major AE peaks. The above-mentioned positive SRS can then be explained. Generally speaking, deformation twinning tends to be apparent under high strain rate. In other words, the higher the strain rate is applied, the more twins will be produced, and the more intensified interaction between twins and mobile dislocations will be. Thus, higher tensile strength is possible under higher strain rate. In addition, CRSS of basal slip is a little positively dependent on strain rate. Therefore, combined hardening effect of both basal slip and twinning may overweigh softening effect of DSA, and the net output will still remain positive. As far as as-received LA11 is concerned, because PLC phenomenon is absent and the influence of DSA is insignificant, larger hardening effect is expected (Fig. 6).

Annealing induced twins

Though twins are produced after annealing, AE peak values of annealing LA41 are appreciatedly lowered. A big difference must lie between the role of deformation-induced twins and that of annealing induced twins. It is believed that the reduction of AE peak values, e.g. from 8.89 mV (as-received LA41) to 4.19 mV (annealed LA41) at the strain rate of $1.11 \times 10^{-4}s^{-1}$, is mainly caused by pre-existing annealing-induced twins. Such kind of twins will obstruct normal movement of mobile dislocations and shorten effective flight distance between obstacles. Consequently, the AE activity will be reduced. Additionally, DSA will not be active because the interaction between mobile dislocations and solute atoms will be decreased. Accordingly, collective motion of mobile dislocations is impossible and the PLC effect is absent.

Conclusions

(1) Serrated flow was observed in as-received LA41 alloy, while it was absent in as-received LA11. Dynamic strain aging was applied to the explanation of PLC effect. Strain rate sensitivity of the investigated alloys was positive.

(2) Intense AE activity was detected during plastic deformation of two extruded Mg–Li–Al alloys. For all of the tested specimens, major AE peaks were found rightly after yielding points, indicating intense activity both of basal and potential secondary slip systems. Beside, due to the fact that dependence of V_{rms} upon $\dot{\varepsilon}^{1/2}$ does not follow an exact linear relationship, and through effective microscope examination, it is suggested that twinning induced by tension plays a significant role in the whole process of deformation. Minor AE bursts had one-to-one correspondence with serrations on the stress–strain curves. AE peak values of as-received LA41 were higher than those of as-received LA11.

(3) Serrations disappeared after 240-h annealing. The reduced value of major AE peak, disappearance of serrations can be elucidated based on the negative effect of preexisting twins, which obstruct normal movement of mobile dislocations, shorten effective flight distance between obstacles and consequently, decrease the AE response.

Acknowledgements The authors would like to thank NSFC (Grant No. 50371089) for financial support, and Dr. W. Tang, Dr. W. Qiu, Prof. L. Liu and Prof. G. Z. Gao for valuable discussions. Special appreciation is dedicated to Prof. X. Q. Wu for constructive suggestions.

References

1. Le Chatelier F (1909) Rev Metall 6:914
2. Cottrell AH, Bilby BA (1949) Proc Phys Soc London A 62:49
3. McCormick PG (1972) Acta Metall 20:351
4. van den Beukel A (1975) Phys Stat Sol (a) 30:197
5. van den Beukel A (1980) Acta Metall 28:965
6. Korbel A, Zasadzinske J, Sieklucka Z (1976) Acta Metall 24:919
7. Schoeck G (1984) Acta Metall 32:1229
8. Kovacs Z, Lendvai J, Voros G (2000) Mater Sci Eng A 279:179
9. Lebyodkin M, Dunin-Barkowskii L, Brechet Y, Estrin Y, Kubin LP (2000) Acta Mater 48:2529
10. Hahner P, Rizzi E (2003) Acta Mater 51:3385
11. Chihab K, Estrin Y, Kubin LP, Vergnol J (1987) Scripta Metall 21:203
12. ASM international, Metals Handbook, Ninth Edition, 17 (1989) 278
13. Lamark TT, Chmelik F, Estrin Y, Lukac P (2004) J Alloy Compd 378:202
14. Friesel M, Carpenter SH (1984) J Acoustic Emission 3:11
15. Mathis K, Chmelik F, Trojanova Z, Lukac P, Lendvai J (2004) Mater Sci Eng A 387–389:331
16. Chmelik F, Moll F, Kiehn J, Mathis K, Lukac P, Kainer KU, Langdon TG (2002) J. Acoustic Emission 20:108
17. Bohlen J, Chmelik F, Dobron P, Kaiser F, Letzig D, Lukac P, Kainer KU (2004) J Alloy Compd 378:207
18. Bohlen J, Chmelik F, Dobron P, Letzig D, Lukac P, Kainer KU (2004) J. Alloy Compd 378:214
19. Bohlen J, Chmelik F, Kaiser F, Letzig D, Lukac P, Kainer KU (2002) Kovove Mater 40:290
20. Dobron P, Chmelik F, Bohlen J, Letzig D, Kainer KU (2005) Kovove Mater 43:193
21. Mulford RA, Kocks UF (1979) Acta Metall 27:1125
22. Heiple CR, Carpenter SH (1987) J Acoustic Emission 6:177
23. Yoo MH (1981) Metall Trans A 12:409
24. Toronchuk JP (1977) Mater Eval 35:51
25. Fisher RM, Lally JS (1967) Can J Phys 45:1147
26. Hauser FE, Landon PR, Dorn JE (1956) Trans ASM 48:986
27. Wang C, Xu YB, Han EH (2006) Acta Metall Sinica 42:191
28. von Mises R, Angew Z (1928) Math Mech 6:85